

See discussions, stats, and author profiles for this publication at: <https://www.researchgate.net/publication/5316019>

Gating of Single Synthetic Nanopores by Proton-Driven DNA Molecular Motors

ARTICLE in JOURNAL OF THE AMERICAN CHEMICAL SOCIETY · AUGUST 2008

Impact Factor: 12.11 · DOI: 10.1021/ja800266p · Source: PubMed

CITATIONS

154

READS

90

12 AUTHORS, INCLUDING:



Fan Xia

Huazhong University of Science and Techn...

58 PUBLICATIONS 3,254 CITATIONS

SEE PROFILE



Wei Guo

548 PUBLICATIONS 3,808 CITATIONS

SEE PROFILE



Xu Hou

Harvard University

31 PUBLICATIONS 1,388 CITATIONS

SEE PROFILE



Yanling Song

17 PUBLICATIONS 342 CITATIONS

SEE PROFILE

Gating of Single Synthetic Nanopores by Proton-Driven DNA Molecular Motors

Fan Xia,[‡] Wei Guo,[†] Youdong Mao,[‡] Xu Hou,[‡] Jianming Xue,[†] Hongwei Xia,[‡]
Lin Wang,[†] Yanling Song,[‡] Hang Ji,[§] Qi Ouyang,[§] Yugang Wang,^{*,†} and Lei Jiang^{*,‡}

State Key Laboratory of Nuclear Physics and Technology, Peking University,
Beijing, 100871, People's Republic of China, Center of Molecular Sciences, Institute of
Chemistry, Chinese Academy of Sciences, Beijing 100190, People's Republic of China, and
Center for Microfluidic and Nanotechnology, Peking University,
Beijing, 100871, People's Republic of China

Received January 24, 2008; E-mail: ygwang@pku.edu.cn; jianglei@iccas.ac.cn

Abstract: Switchable ion channels that are made of membrane proteins play different roles in cellular circuits. Since gating nanopore channels made of proteins can only work in the environment of lipid membrane, they are not fully compatible to the application requirement as a component of those nanodevice systems in which lipid membranes are hard to establish. Here we report a synthetic nanopore–DNA system where single solid-state conical nanopores can be reversibly gated by switching DNA motors immobilized inside the nanopores. High- (on-state) and low- (off-state) conductance states were found within this nanopore–DNA system corresponding to the single-stranded and i-motif structures of the attached DNA motors. The highest gating efficiency indicated as current ratio of on-state versus off-state was found when the length of the attached DNA molecule matched the tip diameter of the nanopore well. This novel nanopore–DNA system, which was gated by collective folding of structured DNA molecules responding to the external stimulus, provided an artificial counterpart of switchable protein-made nanopore channels. The concept of this DNA motor-driven nanopore switch can be used to build novel, biologically inspired nanopore machines with more precisely controlled functions in the near future by replacing the DNA molecules with other functional biomolecules, such as polypeptides or protein enzymes.

Introduction

Numerous kinds of switchable ion channels that are made of membrane proteins play crucial roles in cellular circuits.^{1–4} Many membrane proteins that form nanopore channels may change their conformations between different states. Some of the conformational states allow the channels to conduct certain ions or molecules, while others prohibit the ionic or molecular transport through the channels. Conformational transition between these states is usually referred to as gating.^{3,4} The nanogating device may have important application values in material science. However, as gating of nanopore channels made of proteins can only work in the environment of the lipid membrane, they are not fully compatible with the application requirement as a component of those nanodevice systems in which lipid membranes are hard to establish. This raises the requirement for seeking alternative switchable nanopore machinery. Solid-state nanopores are emerging as an intensively

studied field; they show potential in biomolecular recognition, manipulation, and sequencing.^{5–16} Synthetic nanopores have also been proved to show some gating functions found in biological systems: for example, current rectification. This gating behavior can be modulated by ionic strength,¹⁶ high-valent metal ions, etc.¹² Meanwhile, the advance of DNA nanotechnology^{17–19} has

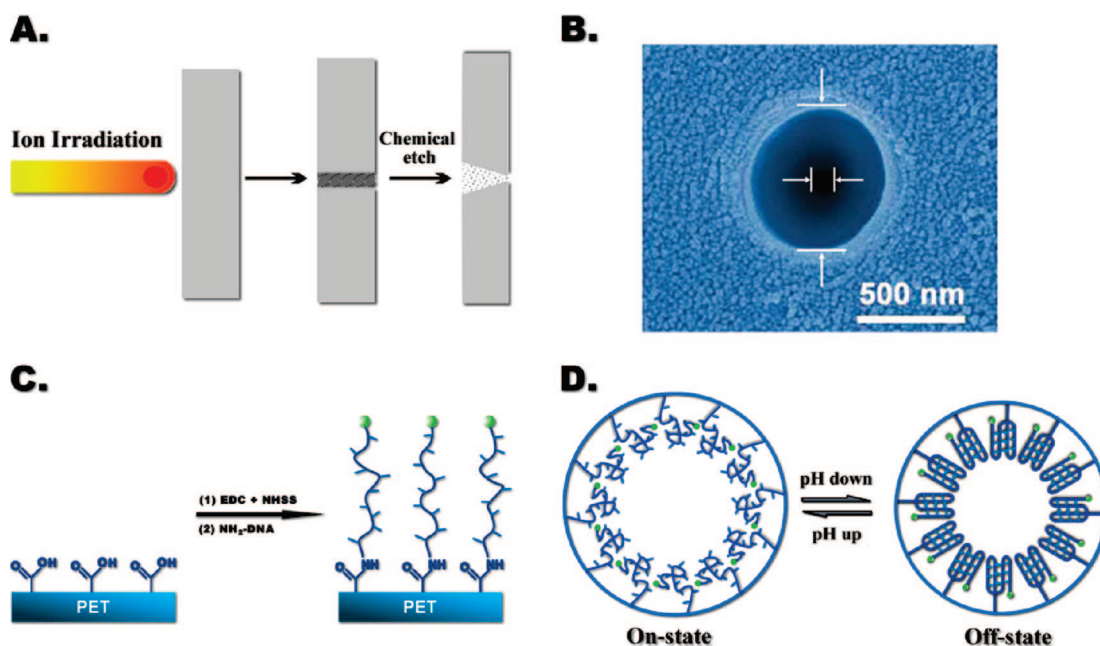
[†] State Key Laboratory of Nuclear Physics and Technology, Peking University.

[‡] Institute of Chemistry, Chinese Academy of Sciences.

[§] Center for Microfluidic and Nanotechnology, Peking University.

- (1) Hille, B. *Ion Channels of Excitable Membranes*; Sinauer Associates: Sunderland, MA, 2001.
- (2) MacKinnon, R. *Angew. Chem., Int. Ed.* **2004**, *43*, 4265–4277.
- (3) Perozo, E.; Cortes, D. M.; Somporipisut, P.; Kloda, A.; Martinac, B. *Nature* **2002**, *418*, 942–948.
- (4) Goychuk, I.; Hänggi, P. *Proc. Natl. Acad. Sci. U.S.A.* **2002**, *99*, 3552–3556.

- (5) Li, J.; Stein, D.; McMullan, C.; Branton, D.; Aziz, M. J.; Golovchenko, J. A. *Nature* **2001**, *412*, 166–169.
- (6) Siwy, Z.; Heins, E. A.; Harrell, C. C.; Kohli, P.; Martin, C. R. *J. Am. Chem. Soc.* **2004**, *126*, 10850–10851.
- (7) Striemer, C. C.; Gaborski, T. R.; McGrath, J. L.; Fauchet, P. M. *Nature* **2007**, *445*, 749–753.
- (8) Iqbal, S. M.; Akin, D.; Bashir, R. *Nat. Nanotechnol.* **2007**, *2*, 243–248.
- (9) Dekker, C. *Nat. Nanotechnol.* **2007**, *2*, 209–215.
- (10) Karnik, R.; Duan, C.; Castellino, K.; Daiguji, H.; Majumdar, A. *Nano Lett.* **2007**, *7*, 547–551.
- (11) Heyden, F. H. J.; Bonthuis, D. J.; Stein, D.; Meyer, C.; Dekker, C. *Nano Lett.* **2007**, *7*, 1022–1025.
- (12) Powell, M.; Sullivan, M.; Vlassioudis, I.; Constantin, D.; Sudre, O.; Martens, C. C.; Eisenberg, R.; Siwy, Z. *Nat. Nanotechnol.* **2008**, *3*, 51–57.
- (13) Wang, G.; Bohaty, A. K.; Zharov, I.; White, H. S. *J. Am. Chem. Soc.* **2006**, *128*, 13553–13558.
- (14) Apel, P.; Korchev, Y.; Siwy, Z.; Spohr, R.; Yoshida, M. *Nucl. Instrum. Methods Phys. Res., Sect. B* **2001**, *184*, 337–346.
- (15) Harrell, C. C.; Kohli, P.; Siwy, Z.; Martin, C. R. *J. Am. Chem. Soc.* **2004**, *126*, 15646–15647.
- (16) Schiedt, B.; Healy, K.; Morrison, A. P.; Neumann, R.; Siwy, Z. *Nucl. Instrum. Methods Phys. Res., Sect. B* **2005**, *236*, 109.
- (17) Seeman, N. C. *Nature* **2003**, *421*, 427–431.
- (18) Yan, H. *Science* **2004**, *306*, 2048–2049.

Scheme 1^a

^a (A) Process of nanopore fabrication by ion-track technique. (B) SEM image of the nanopore with no DNA attached from the base side. (C) Immobilization of DNA motor onto the inner wall of the nanopore by a two-step chemical reaction. (D) The DNA motor is 5'-(NH₂)-(CH₂)₆-AAAAAAAAA CCC TAA CCC TAA CCC TAA CCC (Bodipy493/503)-3', whose conformation is responsive to pH.

allowed researchers, by use of DNA molecules, to perform gating functions inside the synthetic nanopores forming the counterparts of those switchable protein nanopores.^{20,21} Harrell et al.¹⁵ demonstrated the first artificial ion channel by “electromechanical” shift of the DNA molecule. Mao et al.²¹ use functional DNA nanostructure to reveal a nonequilibrium gating of DNA nanochannel. In this article, we intended to combine those previous works together to build a novel nanopore–DNA motor hybrid system that is gated by folding and unfolding of the DNA motor,²³ which closely mimics the gating mechanism of the biological ion channels.

Among many types of biochannels, acid-sensing ion channels (ASICs) are cation-selective, ligand-gated ion channels activated by protons and are implicated in many physiological processes such as pain perception, learning, and memory. Biological ASICs have acidic residue pairs as proton-binding sites to detect environmental protons. Once it is activated or desensitized, consequently conformational changes of the correlative membrane proteins take place to open or close the ion pathway. Inspired by this mechanism, we try to veritally realize gating function of a single synthetic nanopore by grafting functional DNA molecules that experience a stimulus-responsive conformational change of the i-motif structure into an extended structure.²³ Here we report a synthetic nanopore–DNA system where single solid-state conical nanopores can be reversibly gated by switching DNA motors^{22–27} immobilized inside the nanopores. This novel nanopore–DNA system provides an artificial counterpart of switchable protein-made nanopore channels, closely mimicking the gating mechanism of acid-sensing ion channels (ASICs) found in nature.²⁸ On the other hand, a low transmembrane potential of tens of millivolts is a

characteristic of most living cells and is essential to the conduction of action potentials in neurons. One most telling example is the Na⁺–K⁺ transport process.²⁹ Thus, we intended to manipulate the nanopore–DNA motor system under relatively low voltage, which is close to a real biological channel.

As shown in Scheme 1, we immobilized the motor DNA into the nanopore fabricated by the well-developed ion-track technique. The nanopore (Scheme 1A) was embedded in a track-etched poly(ethylene terephthalate) membrane (PET, Hostaphan RN12 Hoechst, 12 μm thick, with single ion track in the center).⁶ Chemical etching of the single-ion irradiated foils leads to the formation of single-pore membranes. The track-etching technique allows control over the shape of the pores, and in our experiment the etched single nanopore was conelike. Its large opening (base) was usually several hundred nanometers, and narrow opening (tip) was 5–44 nm. Diameter measurement of the single conical nanopore was conducted with a commonly used electrochemical method.^{6,14} The next step was to immobilize the motor DNA, which have been extensively studied in the field of nucleic acid nanodevices,^{22–27} onto the inner wall of the nanopore by a two-step chemical reaction (Scheme 1C).

(19) Bath, J.; Turberfield, A. *J. Nat. Nanotechnol.* **2007**, *2*, 275–284.

(20) Mao, Y.; Luo, C.; Deng, W.; Jin, G.; Yu, X.; Zhang, Z.; Ouyang, Q.; Chen, R.; Yu, D. *Nucleic Acids Res.* **2004**, *32*, e144.

(21) Mao, Y.; Chang, S.; Yang, S.; Ouyang, Q.; Jiang, L. *Nat. Nanotechnol.* **2007**, *2*, 366–371.

(22) Sharma, J.; Chhabra, R.; Yan, H.; Liu, Y. *Chem. Commun.* **2007**, *5*, 477–479.

(23) Liu, D. S.; Balasubramanian, S. *Angew. Chem., Int. Ed.* **2003**, *42*, 5734–5736.

(24) Leroy, J. L.; Gehring, K.; Kettani, A.; Gueron, M. *Biochemistry* **1993**, *32*, 6019–6031.

(25) Shu, W.; Liu, D.; Watari, M.; Riener, C. K.; Strunz, T.; Welland, M. E.; Balasubramanian, S.; Mckendry, R. A. *J. Am. Chem. Soc.* **2005**, *127*, 17054–17060.

(26) Liu, D.; Bruckbauer, A.; Abell, C.; Balasubramanian, S.; Kang, D.-J.; Klenerman, D.; Zhou, D. *J. Am. Chem. Soc.* **2006**, *128*, 2067–2071.

(27) Mao, Y.; Liu, D.; Wang, S.; Luo, S.; Wang, W.; Yang, Y.; Ouyang, Q.; Jiang, L. *Nucleic Acids Res.* **2007**, *35*, e33.

(28) Jasti, J.; Furukawa, H.; Gonzales, E. B.; Gouaux, E. *Nature* **2007**, *449*, 316–324.

(29) David, L. N.; Michael, M. C. *Lehninger Principles of Biochemistry, Fourth Edition*; W. H. Freeman, & Co.: New York, 2001.

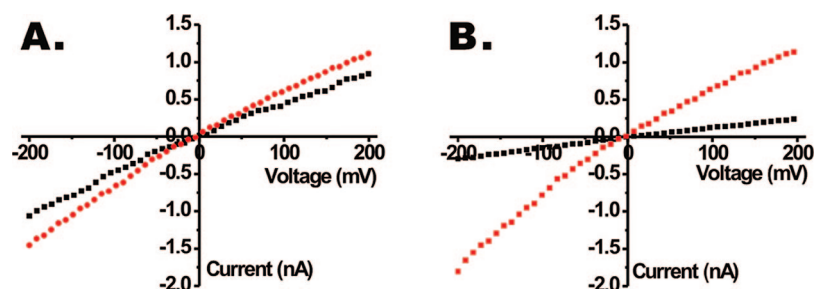


Figure 1. Current–voltage properties of a single nanopore embedded in a PET membrane (A) before and (B) after attachment of motor DNA molecules onto the inner pore wall in PBS solution. I – V characteristics were recorded under symmetric electrolyte conditions at pH 4.5 (black) and 8.5 (red). The diameters of the tip and base are about 17 and 900 nm, respectively.

The motor DNA molecules underwent a pH-response conformational change between a four-stranded i-motif structure (at pH 4.5) and a random single-stranded structure (at pH 8.5) (Scheme 1D).²³

The gating performance of this nanopore–DNA system was evaluated by measuring the ionic current across the channel in environment with variant proton content. Ionic current measurements were carried out with a Keithley 6485 picoammeter (Keithley Instruments, Cleveland, OH) in a custom-designed electrolyte cell with the sample membrane mounted in between. Each half-cell was filled with 2 mL of phosphate-buffered saline (PBS) at pH 4.5 or 8.5. All the experiments herein were conducted at room temperature (about 293 K). Details of nanopore preparation, DNA immobilization, and ionic current measurements are given in the Experimental Section.

Results and Discussion

After the DNA motor assembled onto the inner wall of the nanopore, high- and low-conductance states were found within this artificial ion channel. The potential was stepped in 10 mV steps through the desired potential range, and the resulting transmembrane ion current was measured. Figure 1 shows current–voltage (I – V) curves of a single PET nanopore (A) without any modification and (B) with the motor DNA immobilized in the same nanopore, resulting in the nanopore–DNA system. The transmembrane current was recorded under symmetric electrolyte conditions, for PBS solution at pH 4.5 or 8.5. The low-conductance state emerged in PBS at pH 4.5, and a higher conductive state appeared in PBS at pH 8.5 in both panels of Figure 1. For Figure 1A, charged carboxyl groups (due to the heavy ion irradiation and chemical etching) on unmodified PET surface resulted in some, but very low, difference in ionic current as mentioned in the literature.⁶ Nevertheless, after motor DNA molecules attached onto the inner wall of the nanopore, this difference in ionic current at the two states is remarkably enlarged as shown in Figure 1B. It is known that the DNA molecules are also negatively charged in solution, similarly to the carboxyl groups, which might be responsible for the ionic current difference, similar to the situation in an unmodified PET nanopore. However, there is another important factor that contributed to the remarkably enlarged difference in transmembrane current at low and at high pH. CD experiments in solution clearly showed that the motor DNA molecules experienced reversible conformational change between i-motif conformation at pH 4.5 and extended single-stranded conformation at pH 8.5. Further XPS tests on the PET surface modified with the DNA motor, which were treated with PBS solution at pH 4.5 or 8.5 before the XPS test, confirmed that this DNA molecular motor still worked well after the attachment onto PET surface. (See

both the CD and XPS test results in Supporting Information.) Thus, we attribute this gating behavior of our nanopore–DNA hybrid system to the collective conformational change of the assembled DNA molecular motors. In low-pH (acidic) environment, the DNA motor adopts its rigid quadruplex i-motif structure as a consequence of the formation of intramolecular noncanonical base pairs between cytosine (C) and protonated cytosine (CH^+).^{22–27} Previous atomic force microscopy and electrochemical studies have shown that the i-motif structure can densely pack on a solid-state surface at pH 4.5 but may transition into loosely packed single-stranded structure at pH 8.5 due to the breakdown of the intramolecular C– CH^+ base-pairing.²⁷ The structural transition of DNA motor might well induce a change of effective diameter of the nanopore. The relatively dense packing of DNA molecules with i-motif structure on the inner surface of the pore may efficiently decrease the effective diameter, resulting in low conductivity, while the DNA with single-stranded structure loosely packing on the pore wall cannot efficiently reduce the effective diameter, leading to high conductivity. On the other hand, the extended single-stranded DNA conformation present at pH 8.5, where the backbone of the DNA molecule was highly charged, can help to increase the ionic conductivity near or inside the nanopore tip, similar to the function of the surface charge.

We have also investigated a series of nanopores whose tip diameter spans from 5 to 44 nm. Figure 2 A,B shows the measured current of the nanopore at both pH 4.5 and 8.5. The insets show that the two states exhibit steady current at a constant potential of ± 200 mV. In Figure 2A, it can be seen clearly that the difference between current in high- and low-pH solution was much more distinct within the nanopores with moderate tip diameter of 15–25 nm compared to the rest of the nanopores. If we define high-conductance states as on states and low-conductance states as off states, one can calculate the on–off ratio. We investigated the dependence of the gating efficiency (on–off ratio) of our nanopore–DNA system on the diameters of the pore tip side. As shown in Figure 2A,C, with negative potential, the transmembrane current increased with the tip diameter in both on and off states. However, their ratio reached its maximum in the nanopores with 17 nm tip diameter, and the measured samples whose tip diameters ranging from 15 to 25 nm exhibit much higher on–off ratios between the two states. For comparison, we have also done control experiments on nanopores with no DNA motor immobilization (green columns in Figure 2C). These nanopores with 15–25 nm tip diameter modified with DNA motor have distinctly larger on–off ratios than before DNA motor attachment. If the tip diameter of the nanopore is too small, substantial spatial overlap will occur for counteroriented single-stranded DNA, whose

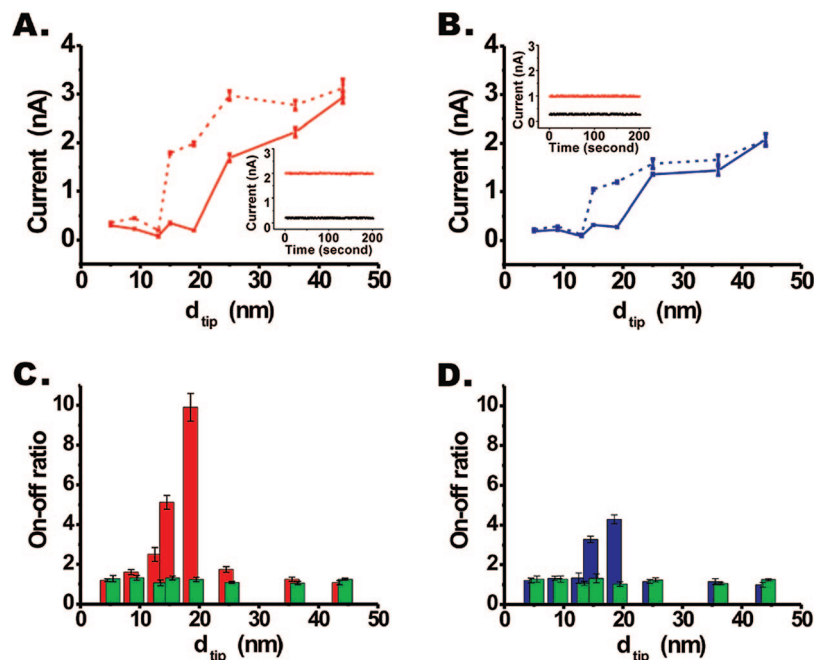


Figure 2. (A, B) Measured current of nanopore–DNA motor system, off-state current at pH = 4.5 (solid lines) and on-state current at pH = 8.5 (dashed lines). The applied external voltage was (A) -200 mV or (B) $+200$ mV, with anode applied to the base side of the nanopore. (Inset) Examples of current–time curves demonstrate that both states exhibited steady current at the working potential of ± 200 mV. (C, D) Current ratio of on state versus off states (on–off ratio) calculated in the nanopore–DNA system with (C) negative potential -200 mV (red columns) or (D) positive potential $+200$ mV (blue columns), and the control measurements with no motor DNA molecules attached on (green column).

mean length at pH 8.5 is about 10 nm. Severe steric hindrance for the conformational motion of DNA strands causes low efficiency of DNA motor switching at the tip side of the nanopore, thus leading to low efficiency of nanopore gating. It is intuitive that the smaller the pore's diameter is, the stronger the steric hindrance for i-motif formation and relaxation and the lower the on–off ratio. For nanopores with too-large tip diameters, the influence brought by the DNA motor is not prominent and consequently the on–off ratio drops down. When the length of the DNA motor matches the tip diameter well, the nanopore acted as a more efficient switch.

We have further compared the on–off ratio of the nanopore–DNA motor system with negative potential (Figure 2C) and positive potential (Figure 2D). We found that both the magnitude of transmembrane current and the on–off ratio decreased at positive potential compared to those at negative potential. The conformational change of the DNA motor induces different steric hindrance and charge redistribution inside the nanopore. The rigid i-motif structure was assumed to be densely packed and less charged; therefore it partly reduces the effective diameter of the nanopore and is not markedly shifted by the external field. According to former studies on the role of surface charge on the conical nanopore wall,⁶ the negative surface charge can increase the ionic concentration near or inside the nanopore tip at negative potential,^{30,31} and therefore the total transmembrane current. DNA chains are also negatively charged in solution and they may extend toward the anode, especially when they adopt loose structure at pH 8.5.¹⁵ When the anode is located on the pore tip side (negative potential), the negatively charged DNA chains confined in a narrow region near the pore tip would

consequently increase the transmembrane current and therefore the on–off ratio.⁶ For seeking a higher flux and better performance of the nanopore–DNA system, we prefer to use the negative potential to operate the nanopore machine.

Besides the pH-sensitive DNA motor molecules, regular DNA whose conformation is not sensitive to pH may also be pH-gated³² since DNA is less charged at low pH and more charged at high pH. Here, we select the poly-A-DNA whose conformation is not sensitive to pH (see both CD and XPS test results in Supporting Information for details). Figure 3 showed I – V curves of a single PET nanopore (A) without any modification and (B) after immobilization of the poly-A-DNA in the same nanopore, giving the nanopore–poly-A-DNA hybrid system, recorded under symmetric electrolyte conditions, for pH 4.5 or 8.5. Similar to Figure 1A,B, high-pH solution corresponds to high conductance and low-pH solution leads to low conductance, but the difference is not so distinct as that shown in Figure 1A,B. We also investigated the dependence of the gating efficiency of nanopore–poly-A-DNA on the diameters of the pore tip side. As shown in Figure 3C,D, all the nanopores modified with poly-A-DNA, whose tip diameters range from 9 to 41 nm, have an on–off ratio a little bit higher than the control group (green columns in Figure 3C,D) and much lower than their counterparts, modified with motor DNA molecules shown in Figure 2. The ratio in negative potential is also a little bit higher than the ratio in positive potential that is consistent with the interpretation of the situations in Figure 2C,D. Therefore, the conformational change exhibited in motor DNA molecules indeed contributes to the high on–off ratio in the nanopore–DNA system.

As a nanoswitch, the response time is of great importance to evaluate the overall performance of the device. We have measured the response time of this nanopore–DNA system and illustrated the main results in Figure 4. The motor DNA modified

(30) Liu, Q.; Wang, Y.; Guo, W.; Ji, H.; Xue, J.; Ouyang, Q. *Phys. Rev. E* **2007**, *75*, 051201.

(31) Cervera, J.; Schiedt, B.; Neumann, R.; Mage, S.; Ramirez, P. *J. Chem. Phys.* **2006**, *124*, 104706.

(32) Siwy, Z. S. *Adv. Funct. Mater.* **2006**, *16*, 735.

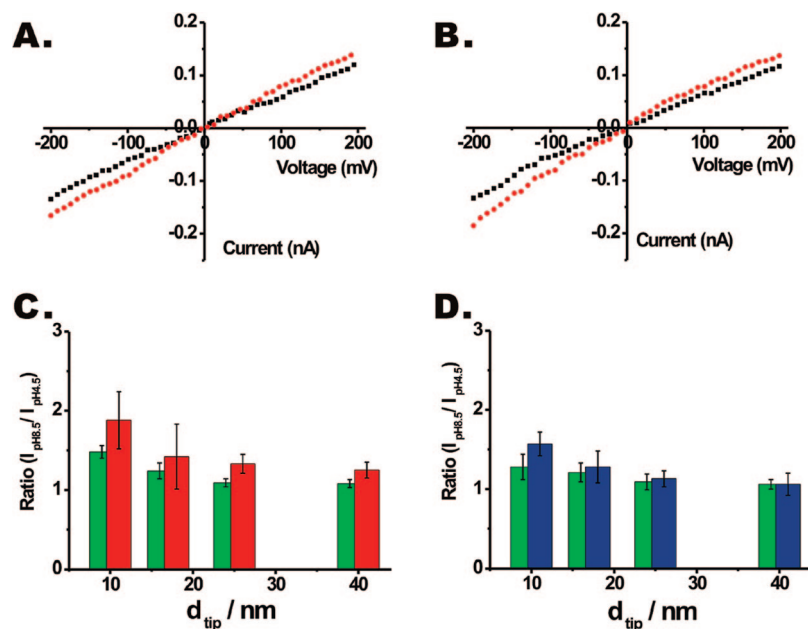


Figure 3. (A, B) Current–voltage properties of a single nanopore embedded in a PET membrane (A) before and (B) after poly-A-DNA molecules attachment onto the inner pore wall in PBS solutions. I – V characteristics were recorded under symmetric electrolyte conditions at pH 4.5 (black) or 8.5 (red). The diameters of the tip and base are about 16 and 900 nm, respectively. (C, D) Current ratio of on versus off states obtained in the nanopore–poly-A-DNA system with (C) negative potential at -200 mV (red columns) or (D) positive potential at $+200$ mV (blue columns), and the control samples (green columns).

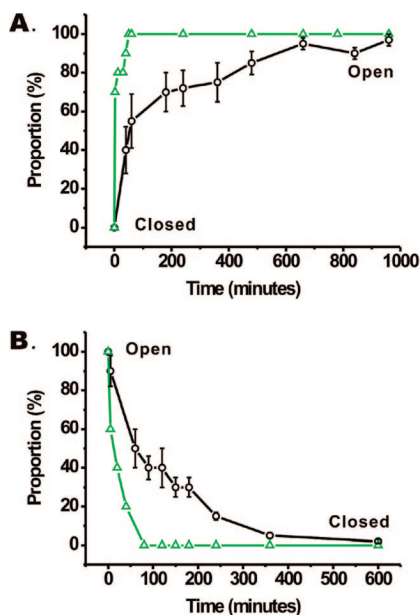


Figure 4. Proportion–time curves of the artificial ion channels at -200 mV. (A) Transition curves from off state (pH 4.5) to on state (pH 8.5); (B) transition curves from on state to off state. Response time curves are shown for nanopore modified with DNA motor (black lines) and for unmodified nanopores (green lines).

nanopore system has an asymmetric and much longer response time for about 600 (off–on time, Figure 4A) and 300 min (on–off time, Figure 4B) than the unmodified nanopores. The CD experiment showed that the DNA molecules in solution experience reversible conformational change between i-motif conformation and extended conformation and inverse in about several minutes (see Supporting Information). We attributed this longer response time of nanopore modified with DNA motor to the collective motion of the DNA molecules in a quite confined region near the pore tip, which is like the case in

biological ion channels³³ where the gating proteins works cooperatively in a confined region, except that the gating proteins operate exceedingly rapidly. Similarly, according to our previous work,²⁷ the switch rate might be accelerated by either modulating the ionic strength in PBS solution or adjusting the environmental temperature. Detailed discussion concerning this topic will be appeared in a separate paper later. In addition, this asymmetrical response behavior was consistent with the results obtained on a separate PET surface (see Supporting Information for detail).

Conclusion

In this article, we demonstrated a novel mechanism that can be used to gate a synthetic nanopore by folding and unfolding some biomolecules. The pH-sensitive DNA molecular motor was attached into the synthetic nanopore. In low-pH solution, the motor DNA folds into a densely packed rigid quadruplex i-motif structure that partially decreases the effective diameter of the nanopore. In high-pH solution, the motor DNA relaxes to a loosely packed single-stranded and more negatively charged structure that enhances the total ion conductivity inside the nanopore. We consider the low and high conductive states as the off and on states of the nanopore–DNA hybrid system. The gating mechanism resembles ASICs found in nature, which are cation-selective, ligand-gated, activated by protons, and participate in many physiological processes such as pain perception, learning, and memory.²⁸ Since DNA motors have been successfully applied to gating of the single nanopore, other responsive molecules such as PNIPAAm and spiropyran should also be future candidates for designing thermo- or light-gated nanopores. In future research work, more complicated biomolecules, such as polypeptides and protein enzymes, may be used

(33) Gillespie, D.; Boda, D.; He, Y.; Apel, P.; Siwy, Z. S. *Biophys. J.* **2008**, doi 10.1529/biophysj.107.127985.

to build novel, biologically inspired nanopore machines with more precisely controlled functions.

Experimental Section

Nanopore Fabrication and Characterization. Poly(ethylene terephthalate) (PET, 12 μm thick) film was irradiated with single swift heavy ion (Au) of energy 11.4 MeV/nucleon at the UNILAC linear accelerator (GSI, Darmstadt, Germany). The film samples were subsequently chemical etched from one side with 9 M NaOH while the other side of the film was in contact with acidic stopping solution in a custom-designed etching cell at room temperature (about 298 K) to form a conical pore. An electrostopping mechanism^{12,13} was employed to protect the tip side of the formed pores from being overetched after breakthrough. The etched membrane was then soaked in MilliQ water (18.2 M Ω) to remove residual salts. The large opening of the cone-shaped nanopore was called base, while the small opening was called tip. The diameter of the base was estimated from the bulk etch rate measured in parallel etching experiments. The tip diameter was evaluated by an electrochemical measurement of the ionic conductance of the nanopore filled with 1 M potassium chloride solution as electrolyte via

$$d_{\text{tip}} = \frac{4LI}{\pi k(c)UD} \quad (1)$$

where d_{tip} is the tip diameter, D is the base diameter, and $k(c)$ is the special conductivity of the electrolyte. For 1 M KCl solution at 25 $^{\circ}\text{C}$ is 0.111 73 $\Omega^{-1}\text{cm}^{-1}$. L is the length of the channel, which could be approximated to the thickness of the membrane after chemical etching. U and I are the applied voltage and measured ionic current in the pore conductivity measurement, respectively. In this work, the base diameter were usually several hundreds nanometers and the tip diameters were from 5 to 44 nm.

DNA Immobilization. The amino single-stranded motor DNA [5'-(NH₂)-(CH₂)₆-AAAAAAAAA CCC TAA CCC TAA CCC TAA CCC (Bodipy493/503)-3'] on the 5' end and poly-A-DNA [5'-(NH₂)-(CH₂)₆-AAAAAAAAA AAA AAA AAA AAA AAA AAA AAA (Bodipy493/503)-3'] on the 5' end were immobilized onto the PET surface and inner pore wall by a two-step chemical reaction as illustrated in Scheme 1C. The NHSS ester was formed by exposure of the single-pore-contained PET film to an aqueous solution of 15 mg EDC and 3 mg NHSS for 1 h. These PET-NHSS ester monolayers were reacted for 2 h with a solution of 1 μM DNA in an alkaline PBS buffer (pH 8.5). After reaction with DNA, some of the NHSS byproduct was removed by soaking in pH 12.2 NaOH for 15 min. And the PET film had been stored for 1 day in alkaline PBS buffer (pH 8.5) before further experiments were carried on.

Current–Voltage Recordings of a Single Nanopore System. The nanopore conductivity and gating properties of the DNA molecules to the nanopore were studied by measuring the ionic current through the unmodified or DNA-modified nanopores. The ionic current was measured by a Keithley 6485 picoammeter (Keithley Instruments, Cleveland, OH). A single-pore PET membrane was mounted between two chambers of the etching cell mentioned above (see Supporting Information). Ag/AgCl electrodes were used to apply a transmembrane potential across the film. The potential difference was calculated as $V_{\text{base}} - V_{\text{tip}}$, where V_{base} and V_{tip} were the potential applied on the base side and on the tip side. The main transmembrane potential used in this work was a scanning voltage varied from -200 to $+200$ mV with its period of 100 s. For comparison,

see Supporting Information, where a higher transmembrane potential with the magnitude of 2000 mV was used. To test the stability of the transmembrane current, constant potentials of -200 and $+200$ mV were applied on the nanopore system for 200 s.

All ionic current recordings were performed with PBS solution at pH values equal to 4.5 and 8.5.^{25–27} The PBS solution is a commonly used pH buffer used in chemical and biochemical experiments made by combining a particular ratio of potassium dihydrogen phosphate (KH₂PO₄) and potassium hydrogen phosphate (K₂HPO₄) and sodium chloride (NaCl) solutions. The cationic strength in both PBS solutions were maintained at 0.1 M K⁺ and 0.1 M Na⁺.

We have measured the current–voltage characteristics on three kinds of nanopore systems: unmodified PET nanopores, motor DNA modified nanopores, and nonresponsive DNA modified nanopores. The process and conditions of all the measurements mentioned in this article are the same, if no particular instructions are added on.

Measurement of the Response Time of the Nanopore–DNA Hybrid System. In this work, the synthetic nanopore was gated by the collective folding and unfolding of the motor DNA molecules that were immobilized in the nanopore. Thus, the response time of the combined nanomachine is equivalent to the transition time between the separate conformations of the motor DNA molecules. In solution phase, the conformational change occurred simultaneously as the environmental pH value changed.³⁴ However, on the surface, this transition time extended to several hours (see Supporting Information). To identify this response time of the DNA molecules confined in the nanopore, we applied a transmembrane potential of -200 mV to measure the current after the environmental pH changed. The temperature was maintained at 298 K and a seal was applied on the cell during the intervals to protect the PBS solution from being vaporized. The current difference in each step was divided by the total change of the current between the two states (PBS solution at pH values 4.5 and 8.5), in which way the current change proportion in each time step could be obtained. The data concerning the response time of the motor DNA modified nanopores shown in this article was summarized over two separate samples whose tip diameters were 11 and 14 nm. We have also measured the current response of unmodified nanopores. Detailed results and discussion can be found in Results and Discussion section.

Acknowledgment. We thank the Material Science Group of GSI, Darmstadt, Germany, for providing the ion-irradiated samples. This work was supported by the National Nature Science Foundation of China (10634010, 10675009, 10675011, 50703020, 20125102, 90306011, and 20421101) and MOE (Grant 306018). We thank Professor. Liu Dongsheng and Dr. Liu Huajie (National Centre for Nanoscience and Technology, Beijing 100080, People's Republic of China) for beneficial discussions.

Supporting Information Available: Synthetic procedures, XPS test, CD spectra of the DNA molecule, and characteristic test of track-etched PET film with DNA. This materials is available free of charge via the Internet at <http://pubs.acs.org>.

JA800266P

(34) Somers, R. C.; Bawendi, M. G.; Nocera, D. G. *Chem. Soc. Rev.* **2007**, 36, 579.